Nonstationary fluctuation analysis and direct resolution of single channel currents at postsynaptic sites

Hugh P. C. Robinson, Yoshinori Sahara, and Nobufumi Kawai
Department of Neurobiology, Tokyo Metropolitan Institute for Neurosciences, Fuchu-shi, Tokyo 183, Japan

ABSTRACT In order to measure unitary properties of receptor channels at the postsynaptic site, the noise within the decay phases of inhibitory postsynaptic currents (IPSCs) and of *N*-methyl-D-aspartate (NMDA)–dependent excitatory postsynaptic currents (EPSCs) in rat hippocampal neurons was studied by nonstationary fluctuation analysis. Least squares scaling of the mean current was used to circumvent the wide variation in amplitude of postsynaptic currents. The variance of fluctuations around the expected current was analyzed to calculate single channel conductance, and fluctuation kinetics were studied with power spectra. The single channel conductance underlying the IPSC was measured as 14 pS, whereas that underlying the EPSC was 42 pS. Openings of the EPSC channel could also be resolved directly in low-noise whole-cell recordings, allowing verification of the accuracy of the fluctuation analysis. The results are the first measurements of the properties of single postsynaptic channels activated during synaptic currents, and suggest that the technique can be widely applicable in investigations of synaptic mechanism and plasticity.

INTRODUCTION

Single channel patch recording is not presently feasible at the intact postsynaptic site, owing to its small size and covering by presynaptic membrane. It is thus difficult to assess the functional correspondence of postsynaptic channels, activated during synaptic currents by their endogenous agonists, to channels activated by artificial applications of agonist. In the case of skeletal muscle nicotinic acetylcholine receptor, the best-characterized transmitter-activated channel, measurements of current fluctuations produced by agonist application at junctional and extrajunctional sites have suggested that junctional channels have a larger single channel conductance (Neher and Sakmann, 1976) and faster burst kinetics (Fishbach and Schuetze, 1980), apparently the result of an exchange of the γ subunit for the ϵ subunit in the channel (for review see Steinbach, 1989). In vertebrate central neurons, glutamatergic excitatory synapses and glycine- or GABA-ergic inhibitory synapses predominate. At these synapses, there may be no clear distinction between synaptic and extrasynaptic channels (Faber et al., 1985). Single channel recording of glutamate receptor-activated channels has revealed seven or more different unitary conductance levels activated by glutamate, via at least three types of receptor, but which subsets of these conductance levels correspond to discrete channel types is still unclear (Nowak et al., 1984; Ascher and Nowak, 1988; Cull-Candy et al., 1988; Jahr and Stevens, 1987; Tang et al., 1989; Lerma et al., 1989; see Collingridge and Lester, 1989, for a review). Postsynaptic currents (PSCs) mediated by NMDA receptors (Forsythe and Westbrook, 1988; Jones and Baughman, 1988) are presumed to arise from openings of channels similar or identical to the relatively distinctive 40–50 pS NMDA-activated channel seen in single channel recording studies, because they share the properties of magnesium block and high calcium permeability. Conductance levels activated preferentially by non-NMDA agonists range from 140 fS up to 35 pS, and the identity of the channel underlying the characteristically fast non-NMDA PSCs is unknown, although Tang et al. (1989) have recently argued that a 35 pS, rapidly desensitizing and quisqualate-preferring channel has the requisite properties for a synaptic channel. GABA and glycine both produce openings to four or five different unitary conductance levels in single channel patch recordings, but there is good evidence that these correspond to a single type of channel molecule (Bormann et al., 1988).

There remain certain basic questions, therefore, concerning the mechanism of glutamatergic and inhibitory synapses in mammalian central neurons. Which, if any, of the channel types revealed by single channel recording studies are operative at the synapse? How many channels function at individual synaptic terminals? How are the time course and amplitude of synaptic current determined by channel kinetic properties and by the form of transmitter release? Definitive answers to such questions will depend on the capability of measuring the

Address correspondence to Dr. Hugh P. C. Robinson, Tokyo Metropolitan Institute for Neurosciences, Fuchu-shi, Tokyo 183, Japan.

unitary properties of the channels activated during synaptic currents.

We have approached this problem in two ways. Firstly, we have studied PSCs using nonstationary fluctuation analysis, which has previously been used for studying single channel properties of voltage-activated sodium channels (Sigworth, 1977, 1980; Conti et al., 1980), and potassium channels (Bennett et al., 1989), and acetylcholine receptor channels activated by fast agonist perfusion (Dilger and Brett, 1990). Unlike the nonstationary currents already studied, however, successive PSCs characteristically display large variations in scale or peak height. In this paper, we examine EPSCs and IPSCs in rat hippocampal neurones, and describe a method for effectively differentiating the fluctuations due to postsynaptic channel gating from those due to presynaptic factors, thus allowing single channel conductance and the kinetics of gating fluctuations to be measured. Secondly, we were able to resolve channel openings directly in low-noise whole-cell recordings of NMDA-dependent EPSCs, to provide an independent confirmation of the accuracy of the fluctuation analysis.

MATERIALS AND METHODS

Cell culture

Primary dissociated cultures of rat hippocampal neurons were prepared by methods similar to those described (Jahr and Stevens, 1987). Briefly, whole hippocampi were isolated from neonatal rats, digested in trypsin, and dissociated by trituration, before plating onto poly-L-lysine coated coverslips. The cells were maintained at 37°C, 100% humidity, 7.5% CO_2, in a medium consisting of Dulbecco's modified Eagle's medium with 5% fetal calf serum, 5–40 U/ml of penicillin, 5–40 μg/ml streptomycin. Whole-cell voltage clamp recordings were performed between days 5 and 10 of culture.

Recording

Spontaneous PSCs were recorded in whole-cell voltage clamp using a patch-clamp amplifier with a 10 GΩ feedback resistor and a compensated frequency response flat to over 10 kHz, and sampled at 44 kHz to 16-bit DAT tape with appropriate antialiasing filtering. Series resistance compensation was not employed—the low levels of current recorded and the high cell resistance (typically 1–10 GΩ) gave a maximum error in applied voltage of ~3% at the peaks of the largest PSCs, for a series resistance of 5 MΩ. The time constant of capacitative charging in whole-cell mode was typically < 40 μs. Several precautions were taken to reduce recording noise: heavily Sylgarded borosilicate glass pipettes were sued, solution levels in the bath and pipette were kept as low as possible, and the electrode holder was cleaned frequently with dry gas. An intracellular (pipette) solution of the following composition was used (concentrations in millimolar): CsCl 141, EGTA 5, $CaCl_2$ 0.5, Hepes/Na 10 (pH 7.2). The bath solution contained (millimolar): NaCl 150, KCl 2.8, $CaCl_2$ 0.5, Hepes/Na 10 (pH 7.2). 5 μM picrotoxin was sometimes added to the bath solution in an attempt to reduce background inhibitory synaptic activity in recordings of EPSCs. Magnesium was omitted from the external solution because of its blocking action on NMDA receptor channels (Nowak et al., 1984). Both the chloride (−2 mV) and monovalent cation reversal potentials were close to 0 mV. APV (D-2-amino-5-phosphonovalerate, Tocris Neuramin, Buckhurst Hill, England), CNQX (6-cyano-7-nitroquinoxaline-2,3-dione, Tocris) and strychnine (Tokyo Kasei Kogyo Co., Tokyo, Japan) were dissolved in bath solution and applied by pressure ejection through micropipettes (tip diameter 3–4 μm) to the postsynaptic cell. All experiments were performed at room temperature (23°–25°C).

Analysis

For noise analysis, the signal was replayed through an eight-pole Butterworth filter with a cutoff frequency of 3 kHz (−3 dB), and resampled at 15 or 20 kHz with a 12-bit A/D converter. Subsequent analysis was carried out in double precision (eight-byte) floating point representation. Spontaneous PSCs were aligned in time to the nearest sample, by matching the zero crossings corresponding to the initiation of the rising phase in their convolutions with a second derivative of a Gaussian function (Marr and Hildreth, 1980). A segment of a constant m samples in length was cut for each PSC in a collection from one cell, starting at a small fixed offset before the rising phase of the PSC and ending after several time constants of decay. The ith point in the ensemble average $\bar{\mathbf{I}}$ of n aligned PSCs was calculated as $\bar{\mathbf{I}}_i = 1/n \sum_{j=1}^{n} y_{ji}$, where y_{ji} is the ith sample in PSC j. An appropriate scaled average vector $\mathbf{B}_j = k_j\bar{\mathbf{I}}$ (see text) was formed for PSC j by one-dimensional downhill simplex minimization (Nelder and Mead, 1965) of $\sum_{i=1}^{m} (y_{ji} - k_j\bar{\mathbf{I}}_i)^2$, varying k_j. The fluctuation vectors $\mathbf{F}$ were then isolated by subtraction: $\mathbf{F}_{ji} = y_{ji} - \mathbf{B}_{ji}$, where $\mathbf{F}_{ji}$ is the ith point in the fluctuation vector from PSC j. For variance distribution measurements, values of $\mathbf{F}_{ji}$ were squared and averaged within bins of their corresponding $\mathbf{B}_{ji}$ values (for IPSCs), or averaged over small (< 5 ms) time intervals and, after subtraction of baseline variance, plotted against the average value of $\mathbf{B}_{ji}$ in the interval (for EPSCs).

For spectral analysis, 1,024-point segments were taken from the $\mathbf{F}$ vectors starting at a fixed offset (12.8 ms) after the initiation of the PSC. Segments were Parzen windowed and the one-sided power spectrum computed by a fast Fourier transform. Average spectra of between 30 and 300 segments (PSCs) were calculated, and a corresponding average spectrum of adjacent baseline segments were subtracted. The resulting difference spectrum was not corrected for the power spectrum of the mean time course as described (Sigworth, 1981), because the number of channels in the population could not be measured (see Appendix), although this correction should be small with low open probability. Thus, the Lorentzian component corresponding to the exponential relaxation of mean current was underestimated. In practice, we did not resolve such components, probably both for this reason and because of their low corner frequencies.

Single channel open times were measured by crossing of a 50% threshold between closed and open current levels. Lifetime histograms were fitted by maximum likelihood, correcting for missed short events due to limited resolution as described (Colquhoun and Sigworth, 1983), by accumulating the conditional probabilities of lifetimes, according to the hypothesized probability density function, given that they were longer than a minimum resolvable lifetime.

RESULTS

Spontaneous PSCs were recorded in 31 cultured hippocampal neurons. Cells were selected for recording which apparently received only one or two visible input fibers from other neurons, to limit synaptic input. In addition,

only small (short diameter < 12 μm) pyramidal neurons with three or four thin (≈ 1 μm), short (< 30 μm visible) processes were used, to attempt to achieve the best possible space clamp and recording noise level. Three kinetically distinct types of spontaneously occurring currents, showing the characteristic temporal summation and peak amplitude variability of postsynaptic currents, could be recorded in such cells: (*a*) intermediate (decay time constant τ = 29–35 ms, Fig. 1 *A*); (*b*) slow (τ = 80–100 ms, Fig. 1 *B* and *C*); and (*c*) fast (τ of 3–4 ms) (Fig. 1 C). The fast and slow classes of PSC were most often initiated simultaneously, giving rise to biphasic PSCs, but both were also occasionally observed separately. All types of PSC reversed around 0 mV, as expected because the reversal potentials for both Cl^- and for monovalent cations were close to 0 mV. Spontaneous PSCs were pharmacologically characterized by superfusion of bath solution containing selective antagonists onto the postsynaptic cell. 10 μM strychnine, a concentration which blocks both GABA and glycine responses in hippocampal neurons (Klee, M. R., T. Shirasaki, and N. Akaike, manuscript submitted for publication) caused a reversible disappearance of intermediate τ PSCs (three cells), but was without effect on the fast and slow types. Fast PSCs could be blocked by 10 μM CNQX, a specific non-NMDA receptor antagonist (Honoré et al., 1988), with no discernible effect on the slow type (three cells), whereas slow PSCs were blocked by 30 μM APV, a selective NMDA antagonist, in which fast PSCs persisted (two cells). The effects of CNQX and APV on intermediate τ PSCs were not studied. These results agree well with previous studies in cultured hippocampal neurons, which have demonstrated choloride-dependent IPSCs, inhibited by GABA blockers, with decay τ's of 20–40 ms at room temperature (Segal and Barker, 1984*b*), corresponding to the present intermediate τ PSCs, as well as the distinctively biphasic glutamatergic EPSCs, with non-NMDA (fast) and NMDA (slow) receptor–mediated components (Forsythe and Westbrook, 1988; Bekkers and Stevens, 1989). For both the IPSCs and biphasic EPSCs in the present study, the fastest times to peak observed were ~1 ms

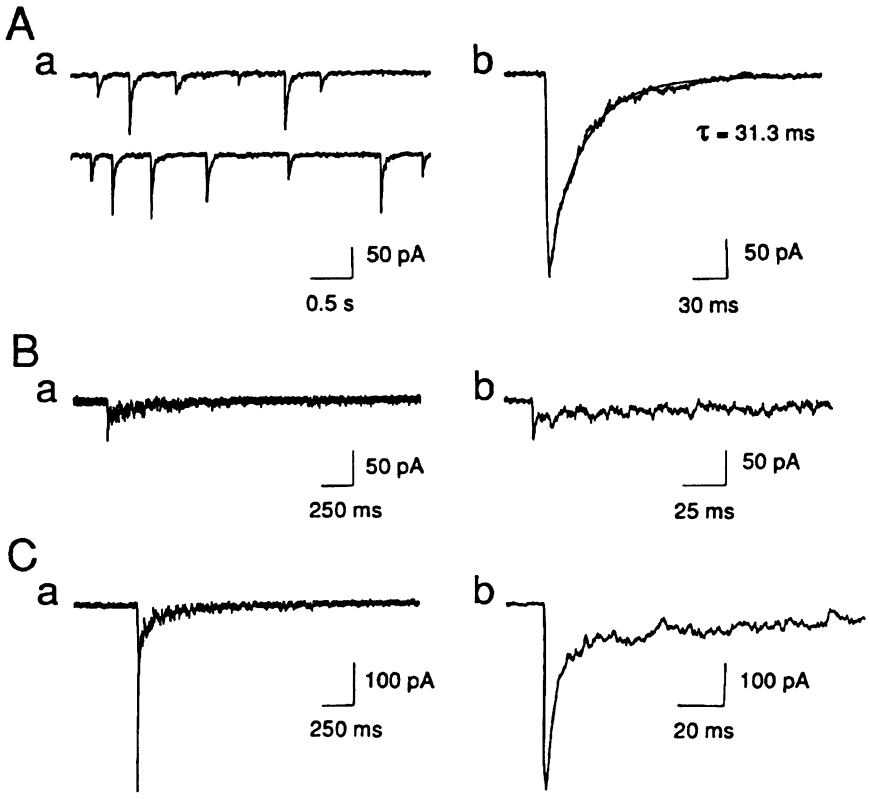

FIGURE 1 Spontaneous PSCs in cultured rat hippocampal neurons. (*A*) Strychnine-sensitive ISPCs, recorded at a holding potential of −70 mV. (*A*, *a*) Two consecutive traces showing IPSCs of various amplitudes. (*A*, *b*) An IPSC at higher time and amplitude resolution, showing a clear increase in fluctuation amplitude during the decay phase. The least squares fit to a single exponential decay is superimposed. (*B*) A monophasic slow (NMDA dependent) EPSC, recorded at −65 mV. (*B*, *a*) At low time resolution, showing the time course of decay over 2.5 s. (*B*, *b*) At higher time resolution, showing the large fluctuations in current over the first 175 ms of decay. (*C*) A biphasic EPSC at (*C*, *a*) low and (*C*, *b*) high time resolutions, recorded at −65 mV. The bandwidth of all records in DC to 3 kHz (−3 dB, eight-pole Bessel).

after the initiation of the PSC. To limit analysis to those PSCs obtained with the best possible space clamp, PSCs with significantly slower times to peak (>2 ms) were not used because they almost surely reflect cable filtering between the synapse and the recording electrode. In extreme cases, such PSCs clearly showed an attenuation of the high frequency fluctuations during decay and therefore appeared artifically smooth.

Unequivocal increases in the noise amplitude over baseline are apparent in the decay phases of the IPSCs and NMDA-type EPSCs (Fig. 1). We assumed that these fluctuations arise from the stochastic gating of the postsynaptic receptor channels, just as such fluctuations are predicted and observed for other macroscopic currents mediated by discrete probabilistic ion channels (for a review see Neher and Stevens, 1977). We therefore attempted to measure the variance and frequency composition of the noise during the decay phase. Channel gating noise in nonstationary macroscopic currents has been examined previously by ensemble fluctuation analysis, where an ensemble mean is calculated by averaging traces, and fluctuations around the mean are calculated by subtraction (Sigworth 1977, 1980), or by taking the differences between pairs of traces, leaving noise distributed around zero with double the power of the fluctuations around the mean (Conti et al., 1980). Such methods are, however, not directly applicable here because the total amount of presynaptic transmitter release varies between successive PSCs, giving rise to a large variation in peak height. We noted that both IPSCs and NMDA-dependent EPSCs could be well fitted by a function $k_j f(t)$, where k_j is a scalar characteristic of the particular PSC and $f(t)$ is the mean time course of the collection of aligned PSCs of identical type. Accordingly, all PSCs in a collection can be scaled and superimposed. This is shown for a collection of IPSCs from one cell, in Fig. 2. Although the collection shows a sixfold variation in peak height (Fig. 2 *A*), when the IPSCs are all normalized to the same peak height, they clearly show the same time course of decay (Fig. 2 *B*). Scaling the mean IPSC (Fig. 2 *C*) allowed it to be closely superimposed on an IPSC whose peak amplitude was quite different from the mean (Fig. 2 *D*). Such invariance of decay kinetics of PSCs of different peak amplitudes is also observed at the muscle endplate (Magleby and Stevens, 1972). Thus, the expected current for a PSC of a particular size—the hypothetical mean current which would result from an ensemble of currents obtained with "identical" conditions of transmitter release—should have the same form as the measured mean current of a collection, but differ only in scale.

To determine single channel properties from macroscopic current noise, we make the usual assumptions

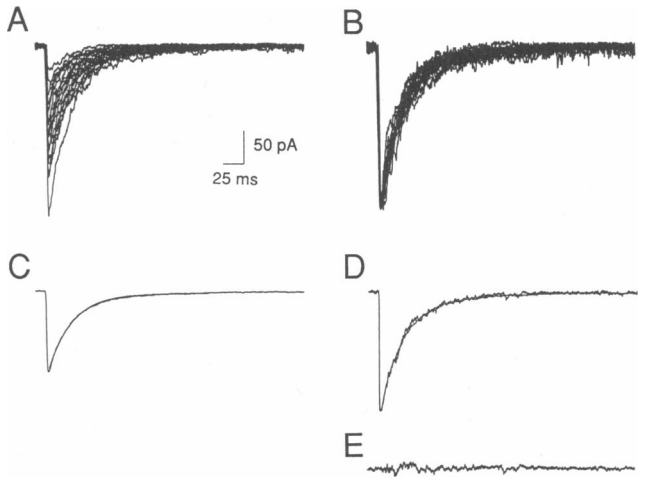

FIGURE 2 Nonstationary fluctuation analysis of PSCs. Scale bars in *A* apply to all of the figure, except for the amplitude scale of *B*. (*A*) 50 IPSCs were recorded at a holding potential of −70 mV and a bandwidth of 3 kHz (−3 dB, Butterworth filter), and aligned by matching their rising phases with an edge detection method. They are plotted superimposed to show the typically wide variation in peak height, in this case from 34 pA to over 250 pA. (*B*) Each PSC in *A* has been scaled to have the same peak height in order to show that kinetics remain unaltered despite the large variations in peak amplitude illustrated in *A*. (*C*) The ensemble average of the 50 PSCs in *A*. (*D*) The ensemble average in *C* was scaled to minimize its squared deviation from one PSC in *A*, and is shown superimposed on the PSC. (*E*) The result of subtracting the scaled ensemble average from the PSC in *D*, consisting of fluctuations around the zero level.

that all channels at a postsynaptic site are identical, independent, and possess a single conducting current level. Furthermore, we assume that opening of a channel is probabilistic, so that after the initiation of an EPSC, each channel has a certain probability of being in the conducting state, $P(t)$. The expected current can therefore be written as $NiP(t)$, where N is the number of functional channels at the postsynaptic site, i.e., the number of channels from which open channels can be stochastically chosen, and i is the single channel current amplitude. For PSCs from the same synaptic site (invariant N), the variation in peak amplitudes is evidently produced by variations in the scale of $P(t)$ (presumably due to varying transmitter release), but effectively without variation in its normalized time course. We can thus write the measured average PSC of the collection as $\bar{I}(t) = Ni\bar{P}(t)$, where $\bar{P}(t)$ is the time course of open probability averaged across a collection of PSCs, and the open probability for a particular PSC, say PSC j, as a constant multiplied by $\bar{P}(t)$: $P_j(t) = k_j\bar{P}(t)$, so that the time course of the expected value of current for that PSC can be written as $I_c(t) = NiP_j(t)$. The variance of fluctua-

tions as a function of the expected current value is then given by the equation (Ehrenstein, 1970; Hille, 1984)

$$\sigma^2 = iI_e - I_e^2/N, \quad (1)$$

which is independent of the form of the open probability as a function of time, and therefore does not assume any particular kinetics.

To measure single channel amplitude from the fluctuations, we sought to estimate $I_e(t)$ for each PSC, measure the fluctuations in a collection of PSCs around particular values of I_e, and use Eq. 1 to fit the resulting distribution, thus obtaining a measure of i. We estimated $I_e(t)$ for each EPSC as $k\bar{I}(t)$ by least-squares fitting of $\bar{I}(t)$ to each EPSC, as described in the Methods. The effectiveness of this heuristic procedure was studied by simulation, as described in the Appendix. The scaled version of the mean PSC which resulted from such least squares fitting was found always closely to estimate the true $I_e(t)$ at low open probabilities. However, model-dependent deviations occur at higher open probabilities, resulting from appreciably long-lived autocovariance in the PSC fluctuations. Therefore, although single channel current is accurately estimated from the initial slopes of variance-current distributions for simulated PSCs, N cannot reliably be measured. There is a further uncertainty in N, because different PSCs included in a collection for fluctuation analysis might originate from different postsynaptic sites, with different N's. This also, however, does not affect the estimate of i from the initial slope of the $\sigma^2(I_e)$ distributions.

An example of a $\sigma^2(I_e)$ distribution for a collection of IPSCs is shown in Fig. 3 A. A curvature, or sublinearity was observed in all IPSC variance-current distributions at higher values of I_e. As discussed in the appendix this probably reflects an artifact of the ensemble average scaling procedure as well as, possibly, the expected

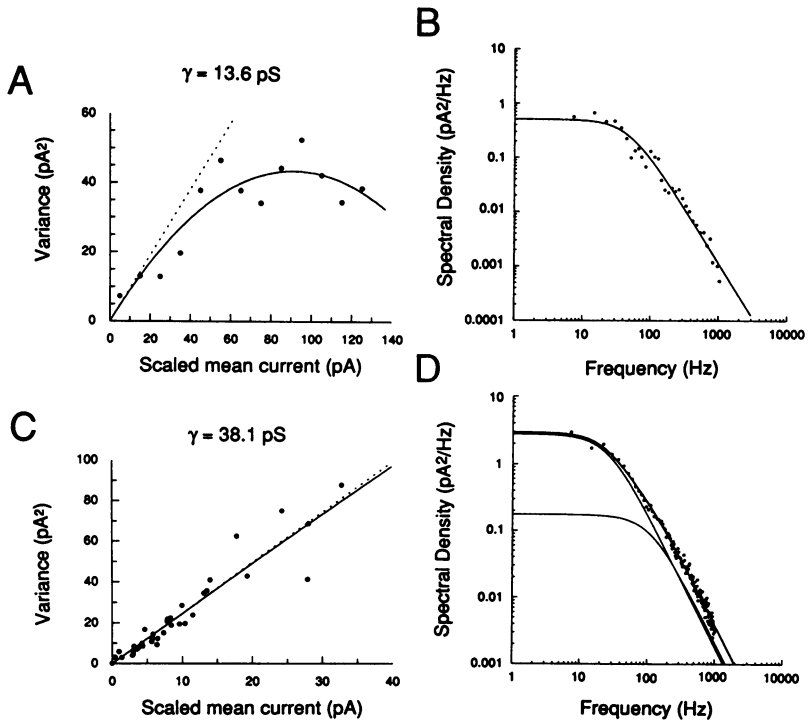

FIGURE 3 Variance and spectral properties of fluctuations in two types of PSC. (*A*) A distribution of current variance as a function of the level of scaled ensemble average current for the IPSCs. The points were fitted with the theoretically expected relation $\sigma^2 = iI_e - I_e^2/N$ (*solid curve*), by nonlinear least squares. The linear zero current asymptote $\sigma^2 = iI_e$, with a slope equal to the predicted single channel current amplitude, is shown as a dotted line. The parameters of the fit are: i = 0.9544 pA, N = 190, giving a γ, assuming reversal at 0 mV, of 13.6 pS. The N value is probably subject to a large error (see Appendix). (*B*) The average power spectrum of the difference fluctuation traces (as illustrated in Fig. 2 *E*), fitted by least squares to a single Lorentzian function (*solid curve*) $G(f) = G_0/(1 + (f/f_c)^2)$, with f_c = 47.2 Hz. This corresponds to an exponential processing of time constant 3.37 ms. (*C*) Variance-current distribution for an ensemble of NMDA-dependent EPSCs, measured at −70 mV. An ensemble of 40 EPSCs were used. Analysis as for *A*, with i = 2.493 pA, N = 779, giving a chord conductance of 38.1 pS. (*D*) Spectrum from the same ensemble as in *C*, fitted to a sum of two Lorentzian functions: $G(f) = G_1/(1 + (f/f_{c1})^2) + G_2/(1 + (f/f_{c2})^2)$, with f_{c1} = 25.4 Hz (τ = 6.25 ms) and f_{c2} = 109.7 Hz (τ = 1.45 ms).

curvature at high open probability. Fits to Eq. 1 (Fig. 3, *A* and *C*), yielded a mean single channel conductance (γ), assuming ohmic behavior and reversal at 0 mV, for IPSCs of 13.9 ± 3.1 pS (±SD, $n = 7$). The NMDA-mediated EPSCs showed no obvious deviation from linear $\sigma^2(I_e)$ distributions at the highest currents measured (Fig. 3 *C*), indicating that the open probability is always low, even at the peak of EPSCs. The single channel conductance was much larger, with an average of 42.2 pS ± 1.6 pS (±SD, $n = 4$).

Power spectra of the fluctuations for the two types of PSC were examined in the frequency range DC to 1,000 Hz. Spectra for IPSCs could best be fit with a single Lorentzian function, of mean corner frequency 40.5 ± 5.4 Hz (±SD, $n = 4$), corresponding to a time constant (τ) of 3.93 ms (Fig. 3 *B*). NMDA type EPSCs consistently showed a sum of two Lorentzians in the same bandwidth (Fig. 3 *D*), one with mean corner frequency at 22.72 ± 3.1 Hz ($\tau = 7$ ms), and the other at 97 ± 11.5 Hz ($\tau = 1.64$ ms, ± SDs, $n = 3$).

The large γ of the NMDA-mediated EPSCs predicts that single channel current transitions should be resolvable in the whole-cell recordings because the single channel current (≈ 3 pA at -70 mV) in some recordings far exceeded the r.m.s. noise level in the baseline (≈ 0.4 pA, 800 Hz Gaussian filter). In EPSCs examined at high gain and reduced bandwidth (Fig. 4 *A* and *B*) these openings were obvious, and were sufficiently well resolved to permit single channel analysis in four cells. Although closed time distributions were not investigated in the present study, the openings displayed a clear burst structure, with groups of closely spaced openings separated by somewhat longer closed times, as observed in extrasynaptic NMDA receptor channels from the same cells (Fig. 4 *B*, *b*). Fitting of amplitude histograms yielded a mean γ of 48.15 ± 4 pS (±SD, $n = 4$), slightly larger than that predicted by the fluctuation analysis. Open lifetime histograms, discarding all events < 2.5 ms due to the level of noise, were fitted to a single exponential probability density function with a time constant of 5.05 ± 0.8 ms (mean ± SD, $n = 3$).

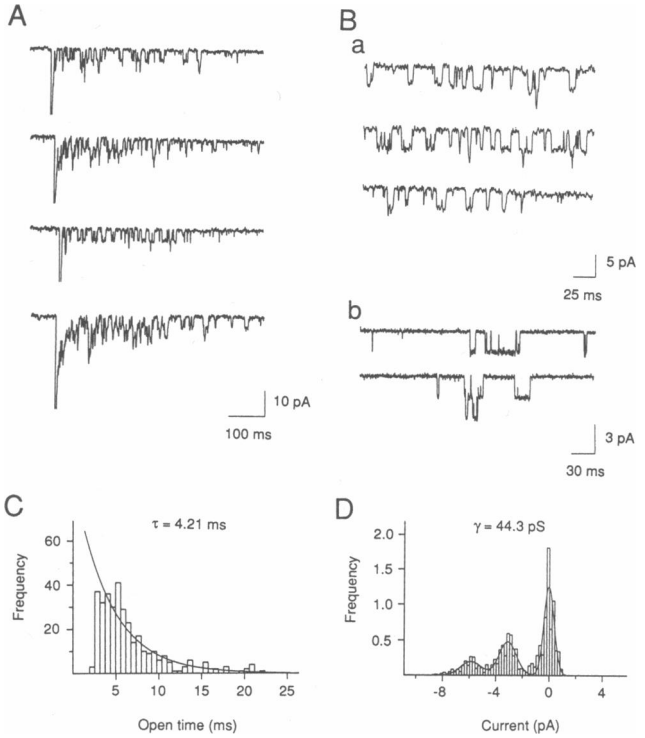

FIGURE 4 Single channel composition of slow EPSCs. (*A*) Four small biphasic EPSCs at high gain, with transitions between one to four discrete open channel levels clearly visible during the slow phase (holding potential −75 mV, filter 800 Hz, −3 dB, Bessel). The peaks of the fast components have been truncated. (*B*, *a*) A view at higher time resolution of segments of the tails of slow EPSCs, showing the burst structure of synaptic channel openings. (*B*, *b*) For comparison, openings (*downwards*) of single NMDA receptor channels (from the same cell culture) recorded in an outside-out patch and activated by 30 μM NMDA + 1 μM glycine in the bathing solution (Potential −46 mV, γ measured as 50.9 pS, filter 2 kHz, −3 dB Bessel). (*C*) Open lifetime histograms of EPSC channels, with a bin size of 0.6 ms and excluding events < 2.5 ms as unreliable. The superimposed curve is the maximum likelihood single exponential probability density function, with missed events correction (see Methods). The number of events is 344, or 623 when corrected for missed events. (*D*) Amplitude histogram of EPSC channels. The amplitudes of individual samples in the tails of EPSCs (later than 100 ms after initiation of the EPSC) were accumulated in bins of 0.2 pA. Frequency is in units of 1,000 samples. The superimposed curve is the least-squares fit to a sum of three Gaussian functions, with peaks at 0, 3.1, and 5.87 pA, corresponding to 0, 1, and 2 open channels, respectively. The amplitude of the first peak yields a γ of 44.3 pS.

DISCUSSION

A potentially serious source of error in these measurements is cable filtering between the synaptic site and the recording electrode, especially in the case of EPSCs where higher frequency components were fitted. However, using the criterion of a time to peak of < 2 ms, we believe that such an error was not significant up to at least 1.5 kHz, for the following reason. A single NMDA-type PSC channel opens effectively instantaneously and can be considered as an ideal step input at the synaptic site. The recorded opening transitions within EPSCs were not discernibly slower than the step response of the recording system passed through the same 1.5 kHz corner frequency Gaussian filter (10–90% rise time of 0.2–0.25 ms), implying that there is no significant additional filtering in this frequency range by the cable structure of the neuron. Similarly, a 1.5 ms time to peak of an IPSC implies, in the worst case (actually instanta-

neous rise), cable filtering approximately equivalent to a 500 Hz corner frequency Gaussian filter.

There are several indications that the fluctuations within the decay phases of the PSCs, as measured here, arise almost exclusively from the stochastic gating of postsynaptic receptor channels. Firstly, the form of the $\sigma^2(I_e)$ distributions is asymptotically linear at low currents, with sublinearity at higher currents in the case of IPSCs, as expected from Eq. 1. Secondly, the power spectra of the fluctuations could be fit with Lorentzian functions, indicative of elementary events of exponentially distributed durations. Thirdly, there is a close correspondence between the measured variance of EPSC fluctuations and that predicted from the properties of the directly resolved channel openings. There seems, therefore, to be no significant source of excess variance. In fact, the measured variance is slightly below that predicted from the directly resolved openings, an effect which probably arises in part from the method of least-squares scaling, as discussed in the Appendix. Another reason for underestimation may be the limited bandwidth in fluctuation measurements. Finally, if there exist subconductance levels of the EPSC channel which are occupied for significant periods of time, the measured γ would be less than the γ of the main conductance state.

Direct resolution of single channel transitions in PSCs requires lower background noise levels than does fluctuation analysis, and is presently applicable only to relatively large single channel conductances. Further reductions in the background noise level during whole-cell single channel recording will be limited not only by cell capacitance and resistance (Marty and Neher, 1983), but also by extraneous channel activity, which we often observed in highly amplified "baselines." Changes in the filling solution or the use of appropriate pharmacological antagonists might reduce such noise.

The properties of single postsynaptic channels measured here may be compared with those of extrasynaptic receptors in mammalian central neurons activated by exogenous agonists. In general, the differences in temperature, permeant ion concentrations, and applied voltages between this study and others are small enough to be considered negligible. Slow EPSCs in this cell type are mediated by NMDA receptors, as shown by their sensitivity to the NMDA-selective antagonist APV (Forsythe and Westbrook, 1988; Bekkers and Stevens, 1989). We determined a mean γ for this type of 42 pS using fluctuation analysis and of 48 pS, using direct single channel recording. The γ of the principal conductance state of the extrasynaptic NMDA-activated channel lies between 40 and 50 pS, in a variety of mammalian neurons (Ascher et al., 1988; Cull-Candy and Usowicz, 1989; Jahr and Stevens, 1987). The EPSC channels thus have conductances typical of NMDA receptor channels. We measured a single exponentially distributed open time distribution with a time constant of 5 ms, from direct resolution of EPSC channels. The corresponding value for single receptor channels activated by NMDA has been reported as 4.7 ms (Nowak et al., 1984) and 5.9 ms (Ascher et al., 1988), and for the same conductance state activated by glutamate, as 5.3 ms (Ascher et al., 1988). Spectra of EPSC noise were fitted with two Lorentzians of mean corner frequencies 23 and 97 Hz. Very similar mean corner frequencies of 23 and 105 Hz have been reported for two-Lorentzian fits of whole-cell NMDA-evoked noise (Cull-Candy et al., 1988). Although the kinetics of NMDA-activated channels are complex, these two Lorentzians probably correspond to two of the longer components of the burst durations (Howe et al., 1988). A Lorentzian component corresponding to the decay time constant of the PSC (corner frequency $\approx$ 1–2 Hz) is not seen in the present spectra, nor is it in previously reported whole-cell NMDA current spectra, perhaps because the corner frequency is too low. Based on the similarities of amplitude and kinetics, it can be concluded that the channels underlying the slow glutamatergic EPSC in cultured hippocampal neurons are functionally very similar or identical to NMDA-activated channels recorded in response to NMDA application to patches or whole cells.

The single channels involved in the IPSC had a measured mean γ of 14 pS, and fluctuations which could be fit with one Lorentzian, of mean corner frequency 40 Hz (τ = 3.9 ms). IPSCs in hippocampal neurons are thought to be mediated by GABA receptors (Segal and Barker, 1984*b*; Collingridge et al., 1984). In extrasynaptic membrane, both GABA and glycine receptors appear to activate the same set of four or five unitary Cl^- conductance levels, though with different frequencies, suggesting that the two types of receptor are coupled to an essentially identical channel (Bormann et al., 1987). The levels range from 10 pS in steps of ~10–12 pS up to 46 pS. If the states can be considered independent from each other, noise variance analysis should yield an average of the conductance levels, each weighted by its frequency of occupation. Whole-cell noise measurements of GABA-activated currents have yielded γ's of around 14, 16, and 20 pS in cultured dorsal root ganglion, spinal cord, and hippocampal neurons, respectively (Ozawa and Yuzaki, 1984; Segal and Barker, 1984*a*). The somewhat smaller γ observed here might be explained if, under the conditions of extremely fast and transient "perfusion" of agonist which exist at the postsynaptic site, openings to the smaller, 10–12 pS level were favored owing to faster activation of this level. Consistent with this, 30 and 46 pS conductance transitions were never directly resolved during IPSCs, despite

sufficiently low background noise levels. Single Lorentzian fits (Segal and Barker, 1984*a*) of GABA-activated noise spectra have corner frequencies close to 7 Hz, significantly different from our value of 40 Hz. However, fitting of two Lorentzians to GABA-activated noise spectra (Ozawa and Yuzaki, 1984) gave corner frequencies of ~3 Hz and of 30–40 Hz, suggesting that the 40 Hz process in IPSC noise corresponds to the higher frequency Lorentzian process activated by GABA application to the whole cell. The 3 Hz component of Ozawa and Yuzaki corresponds well to the kinetics of IPSC decay, but may be underestimated in our spectra.

Fluctuations within fast non-NMDA glutamatergic EPSCs could not be detected under the present conditions. Either the openings of the channels responsible are all too fast to be resolved with the effective bandwidth of recordings, or are too small, or both. Kainate receptors activate a 140 fS conductance, as measured by whole-cell noise analysis (Cull-Candy et al., 1988), as well as larger conductance levels ~1 pS and higher, any of which could be responsible for the fast non-NMDA EPSCs. However, in the present type of fast EPSC, participation of the 35 pS quisqualate-preferring channel proposed as a candidate nonNMDA synaptic channel (Tang et al., 1989), seems unlikely because openings of this channel should have led to much larger current noise and should also have been resolved directly, because of their large size and lifetimes lasting up to 5–10 ms.

Measurement of single postsynaptic channel amplitude and kinetics as described in this investigation is a valuable complement to studies of receptor channels activated by artificial application of agonists, in several ways. Firstly, any substantial differences in the properties of synaptic channels activated during PSCs are likely to have significance for synaptic functions. Differences could be intrinsic to the receptor channel molecule or result from the composition of the endogenous agonist or from presynaptic release of receptor channel modulators. If, on the other hand, it can be established that synaptic channels and artificially-activated channels function identically, as strongly implied here for the NMDA receptor channel, then results on extrasynaptic receptor channels may justifiedly be extrapolated to the synapse. Furthermore, because the population of channels at a synaptic site is well separated from other channels during activation, and probably contains only one or two homogeneous types, synaptic single channel measurements could resolve ambiguities arising from incomplete agonist specificity between several mixed receptor channel subtypes. Finally, a probabilistic description of PSC kinetics at the single channel level will be important at postsynaptic sites of high input resistance such as dendritic spines, where significant voltage noise must result from stochastic channel gating.

APPENDIX

The accuracy of the heuristic procedure of least-squares scaling of the mean PSC to estimate the expected current timecourse was tested with simulated PSCs. A simple model of channel gating was assumed, with one open state and two closed states:

$$C_1 \xleftarrow{k_1} O \underset{k_3}{\overset{k_2}{\rightleftharpoons}} C_2.$$

Once in the open state, a channel may pass to and from the C_2 state a variable number of times (whose distribution depends on the ratio k_2:k_1) before being absorbed to the C_1 state. At zero time, a channel was placed in the open state and its evolution then followed until it reached the absorbing C_1 state. This is equivalent to assuming that the step C_1 to O necessitates the binding of transmitter, and that the release of transmitter at time zero is essentially pulsatile, with instantaneous binding. Lifetimes were calculated as $-(\log_e r)/(k_1 + k_2)$ for the open state, and $-(\log_e r)/k_3$ for the C_2 state, where r is a uniform deviate random number between 0 and 1. To calculate the destination of transitions away from the open state, another r was generated: if it was less than the quantity $k_1/(k_2 + k_3)$, then the transition was to C_1, if greater than or equal, the transition was to C_2. PSCs were constructed by adding simulations of a large number of individual channels. Variation in peak height of PSCs, then, could be produced by variable numbers of channels which 'bound transmitter' (were placed in the open state) at time zero. This type of model reproduces the observed scale invariance of PSC form.

Several example simulated PSCs are shown in Fig. A1 *A a*. Their ensemble average (Fig. A1 *A b*) shows a two exponential decay, as expected, with rates given by the eigenvalues: $\lambda_1 = \frac{1}{2}(-b + \sqrt{b^2 - 4c})$ and $\lambda_2 = \frac{1}{2}(-b - \sqrt{b^2 - 4c})$, where $b = -(k_1 + k_2 + k_3)$ and $c = k_1k_3$.

To investigate the accuracy of the least-squares scaling method in measuring fluctuation variance, variance-current distributions of PSCs simulated using a constant number of channels were calculated by scaling the ensemble average before subtraction to minimize total squared deviation for each PSC. As shown in Fig. A1 *B*, distributions adhered well to the expected form at low I, giving accurate estimates of the single channel amplitude determined from the gradient of the zero current asymptote. However, perhaps somewhat nonintuitively, the distributions diverged at higher I, in a way depending on the rate constants used, making accurate measurements of N impossible. The reason for this is that, inevitably, the scaled ensemble average fits at least slightly better to each PSC, in a total least-squares sense, than does the true expectation current $[NiP(t)]$. In the long-lasting middle range of current, therefore, variance is consistently underestimated, at the expense of deviating from the short-lived peak current regions. The size of the artifact depended on the rate constants used: with k_2 and k_3 high relative to k_1 (openings much shorter than the decay time course), the artifact was small, but increased as k_2 and k_3 were lowered relative to k_1. We investigated ratios of k_2 and k_3 to k_1 from 10 up to 350. Addition of small levels of Gaussian-distributed background noise to PSC traces, to simulate baseline noise, had no effect on the form of current-variance distributions (not shown). A rough indication of the extent of the high-current artifact in analysis of real PSCs can be obtained by comparing the ratio of decay time constant to mean open lifetime for simulated and actual PSCs (the principal time constant of

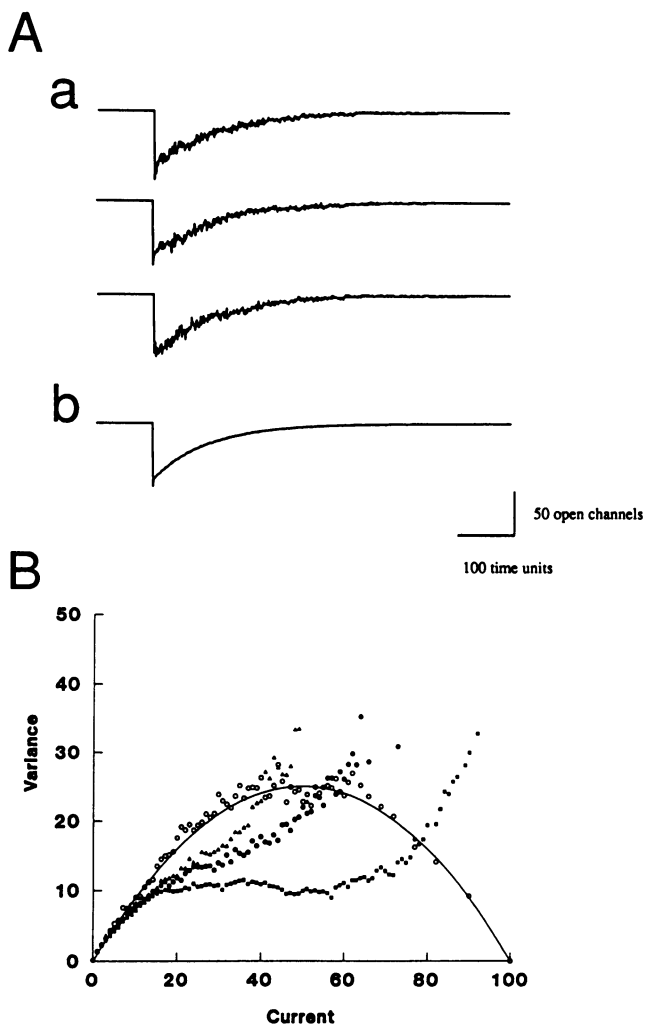

FIGURE A1 Fluctuation analysis of simulated PSCs. (*A*, *a*) Three example PSCs simulated as described in the text, with 100 channels, $k_1 = 0.015$, $k_2 = 0.15$, and $k_3 = 2.0$. (*A*, *b*) The ensemble average of 300 such PSCs. (*B*) Current-variance distributions of simulated PSCs obtained by scaled fits of the ensemble average. For each distribution, 1,000 PSCs were simulated, with 100 channels. The single channel amplitude is equal to one unit of current. Open circles: variance calculated without least-squares scaling of ensemble average prior to subtraction. Solid symbols: variance calculated with least-squares scaling of ensemble average to each PSC. (1) (*triangles*) $k_1 = 0.015, k_2 = k_3 = 2$; (2) (*circles*) $k_1 = 0.015, k_2 = 0.5, k_3 = 1$; (3) (*squares*) $k_1 = 0.015$, $k_2 = 0.15$, $k_3 = 2$. The solid curve is the theoretically expected distribution: $\sigma^2 = I - I^2/100$.

decay was used for simulated PSCs). The three models in Fig. A1 *B* have ratios of 269, 51.7, and 11.83 for curves 1, 2, and 3, respectively. Real EPSCs had a ratio of ~20, and IPSCs of ~8, indicating that IPSCs have a comparable artifact to model 3, whereas the curve for EPSCs lies somewhere between that for models 2 and 3 of Fig. 5 *B*.

These simulations have shown that analysis of PSC noise should preferentially use the tails of the decay phase, rather than the peaks, because of the artifact introduced by the procedure of least-squares scaling of the ensemble average. In both the power spectral analysis and the variance analysis of IPSCs, the first 12.8 ms of each PSC was discarded for this reason.

Because the decay phase of PSCs and of mean PSCs were well-fitted with single exponentials, an alternative method of estimating the expected current might be to fit single exponentials or other smooth functions *ad hoc* to the decay phase of each PSC, as suggested by Sigworth (1981) for nonstationary currents whose ensemble mean cannot be computed due to technical constraints. This method, though, is inferior to using the scaled mean current in the present case, because the latter method constrains each current to have the same normalized time course as the mean current, and thus incorporates information about the expected current averaged over a collection of PSCs. However, *ad hoc* fitting of PSC decay could be useful if the normalized time couse of a homogeneous type of PSCs was observed to vary with peak amplitude.

We thank Prof. N. Akaike and Dr. R. Fettiplace and Dr. Y. Kubo for their comments.

This work was supported by a grant from the Japanese Ministry of Science, Education and Culture (No. 63060006).

Received for publication 5 July 1990 and in final form 24 September 1990.

REFERENCES

Ascher, P., and L. Nowak. Quisqualate- and kainate-activated channels in mouse central neurones in culture. 1988. *J. Physiol. (Lond.).* 399:227–246.

Ascher, P., P. Bregestovski, and L. Nowak. 1988. *N*-Methyl-D-aspartate activated channels of mouse central neurones in magnesium-free solutions. *J. Physiol. (Lond.).* 399:207–226.

Bekkers, J. M., and C. F. Stevens. 1989. NMDA and non-NMDA receptors are colocalized at individual excitatory synapses in cultured rat hippocampus. *Nature (Lond.).* 341:230–233.

Bennett, P. B., R. Kass, and T. Begenisch. 1989. Nonstationary fluctuation analysis of the delayed rectifier K channel in cardiac Purkinje fibers. *Biophys. J.* 55:731–738.

Bormann, J., O. P. Hamill, and B. Sakmann. 1987. Mechanism of anion permeation through channels gated by glycine and γ-aminobutyric acid in mouse cultured spinal neurones. *J. Physiol. (Lond.).* 385:243–286.

Collingridge, G. L., and R. A. J. Lester. 1989. Excitatory amino acid receptors in the vertebrate central nervous system. *Pharmacol. Rev.* 40:143–211.

Collingridge, G. L., P. W. Gage, and B. Robertson. 1984. Inhibitory postsynaptic currents in rat hippocampal CA1 neurons. *J. Physiol. (Lond.).* 356:551–564.

Colquhoun, D., and F. J. Sigworth. 1983. Fitting and statistical analysis of single channel records. *In* Single Channel Recording. E. Neher and B. Sakmann, editors. Plenum Publishing Corp., New York. 191–263.

Conti, F., B. Neumke, W. Nonner, and R. Stampfli. 1980. Conductance fluctuations from the inactivation process of sodium channels in myelinated nerve fibres. *J. Physiol. (Lond.).* 308:217–239.

Cull-Candy, S. G., and M. M. Usowicz. 1989. On the multiple-

conductance single channels activated by excitatory amino acids in large cerebellar neurones of the rat. *J. Physiol. (Lond.)*. 415:555–582.

Cull-Candy, S. G., J. R. Howe, and D. C. Ogden. 1988. Noise and single channels activated by excitatory amino acids in rat cerebellar granule neurons. *J. Physiol. (Lond.)*. 400:189–222.

Dilger, J. P., and R. S. Brett. 1990. Direct measurement of the concentration- and time-dependent open probability of the nicotinic receptor channel. *Biophys. J.* 57:723–732.

Ehrenstein, G., H. Lecar, and R. Nossal. 1970. The nature of the negative resistance in bimolecular lipid membranes containing excitability inducing material. *J. Gen. Physiol.* 55:119–133.

Faber, D. S., P. G. Funch, and H. Korn. 1985. Evidence that receptors mediating central synaptic potentials extend beyond the postsynaptic density. *Proc. Natl. Acad. Sci. USA*. 82:3504–3508.

Fishbach, G. D., and S. M. Schuetze. 1980. A post-natal decrease in acetylcholine channel open time at rat endplates. *J. Physiol. (Lond.)*. 303:125–137.

Forsythe, I. D., and G. L. Westbrook. 1988. Slow excitatory postsynaptic currents mediated by *N*-methyl-D-aspartate receptors on cultured mouse central neurones. *J. Physiol. (Lond.)*. 396:515–533.

Hille, B. 1984. Ionic Channels of Excitable Membranes. Sinauer Associates, Inc., Sunderland, MA. 426 pp.

Honoré, T., S. N. Davies, J. Drejer, E. J. Fletcher, P. Jacobsen, D. Lodge, and F. E. Nielsen. 1988. Quinoxalinediones: potent competitive non-*N*-methyl-D-aspartate glutamate receptor antagonists. *Science (Wash. DC)*. 241:701–703.

Howe, J. R., D. Colquhoun, and S. G. Cull-Candy. 1988. On the kinetics of large-conductance glutamate-receptor ion channels in rat cerebellar granule neurons. *Proc. R. Soc. Lond. B Biol. Sci.* 223:407–422.

Jahr, C. E., and C. F. Stevens. 1987. Glutamate activates multiple single channel conductances in hippocampal neurons. *Nature (Lond.)*. 325:522–525.

Jones, K. A., and R. W. Baughman. 1988. NMDA- and non-NMDA-receptor components of excitatory synaptic potentials recorded from cells in layer V of rat visual cortex. *J. Neurosci.* 8:3522–3534.

Lerma, J., L. Kushner, R. S. Zukin, and M. V. L. Bennett. 1989. *N*-methyl-D-aspartate activates different channels than do kainate and quisqualate. *Proc. Natl. Acad. Sci. USA*. 86:2083–2087.

Magleby, K. L., and C. F. Stevens. 1972. A quantitative description of end-plate currrents. *J. Physiol. (Lond.)*. 223:173–197.

Marr, D., and E. Hildreth. 1980. Theory of edge detection. *Proc. R. Soc. Lond. B Biol. Sci.* 207:187–217.

Marty, A., and E. Neher. 1983. Tight-seal whole-cell recording. *In* Single Channel Recording. Chapter 7. E. Neher and B. Sakmann, editors. Plenum Publishing Corp., New York.

Neher, E., and B. Sakmann. 1976. Noise analysis of drug induced voltage clamp currents in denervated frog muscle fibres. *J. Physiol. (Lond.)*. 258:705–729.

Neher, E., and C. F. Stevens. 1977. Conductance fluctuations and ionic pores in membranes. *Annu. Rev. Biophys. Bioeng.* 6:345–381.

Nelder, J. A., and R. Mead. 1965. A simplex method for function minimization. *Comput. J.* 7:308–313.

Nowak, L., P. Bregestovki, P. Ascher, A. Herbet, and A. Prochiantz. 1984. Magnesium gates glutamate-activated channels in mouse central neurones. *Nature (Lond.)*. 307:462–465.

Ozawa, S., and M. Yuzaki. 1984. Patch-clamp studies of chloride channels activated by gamma-aminobutyric acid in cultured hippocampal neurons of the rat. *Neurosci. Res.* 1:275–293.

Segal, M., and J. L. Barker. 1984*a*. Rat hippocampal neurons in culture: properties of GABA-activated Cl^- ion conductance. *J. Neurophysiol. (Bethesda)*. 51:500–515.

Segal, M., and J. L. Barker. 1984*b*. Rat hippocampal neurons in culture: voltage clamp analysis of inhibitory synaptic connections. *J. Neurophysiol. (Bethesda)*. 52:469–487.

Sigworth, F. J. 1977. Sodium channels in nerve apparently have two conductance states. *Nature (Lond.)*. 270:265–267.

Sigworth, F. J. 1980. The variance of sodium current fluctuations at the node of Ranvier. *J. Physiol. (Lond.)*. 307:97–129.

Sigworth, F. J. 1981. Interpreting power spectra from nonstationary membrane current fluctuations. *Biophys. J.* 35:289–300.

Steinbach, J. H. 1989. Structural and functional diversity in vertebrate skeletal muscle nicotinic acetylcholine receptors. *Annu. Rev. Physiol.* 51:353–365.

Tang, C.-M., M. Dichter, and M. Morad. 1989. Quisqualate activates a rapidly inactivating high conductance ionic channel in hippocampal neurons. *Science (Wash. DC)*. 243:1474–1477.